

Dynamical properties of a nonlinear growth equation

Mohammed Benlahsen^a, Gabriella Bognár^{c,*}, Mohammed Guedda^b, Zoltán Csáti^c, Krisztián Hriczó^c

^a*LPMC, Université de Picardie Jules Verne, Amiens, France*

^b*LAMFA, UMR-CNRS 7352, Université de Picardie Jules Verne, Amiens, France*

^c*University of Miskolc, Miskolc-Egyetemváros 3515, Hungary*

Abstract

The conserved Kuramoto-Sivashinsky equation is considered as the evolution equation of amorphous thin film growth in one- and in two-dimensions. The role of the nonlinear term $\Delta(|\nabla u|^2)$ and the properties of the solutions are investigated analytically and numerically. We provide analytical results on the wavelength and amplitude. We present numerical simulations to this equation which show the roughening and coarsening of the surface pattern and the evolution of the surface morphology in time for different parameter values in one- and in two-dimensions.

Keywords: growth model, molecular beam epitaxy, meandering, coarsening

1. Introduction

Molecular Beam Epitaxy (MBE), which has many important technological and industrial applications, is often used to grow nanostructure on crystal surfaces. The evolution of the surface morphology during MBE growth results from a competition between the molecular flux and the relaxation of the surface profile through surface diffusion of adatoms. One crucial aspect of the growth process is its possible unstable character, due to deterministic mechanisms, which prevent the growing surface to stay parallel to the substrate [1]-[9].

This phenomenon has turned out to be a source of a wide class of nonlinear dynamics, which varies from spatio-temporal chaos [10] to the formation of stable structures [11], from coarsening processes [12] to diverging amplitude structures [13]. One of the many challenges involved in applied mathematics and nonequilibrium physics is to predict the behavior of surface evolution, from the knowledge of an initial arbitrary profile, and the scaling relationships between surface features in various growth regimes. In [14], Frisch and Verga studied the step meandering instability on a surface characterized by the alteration of terraces with different properties as in the case of Si(001). Under the assumption of negligible desorption and Erlich-Schwoebel (ES) effect, the surface morphology is investigated by means of the following unstable mode equation (Conserved Kuramoto-Sivashinsky, CKS for short)

$$\partial_t u = -\partial_x^2 \left[\nu u + \kappa \partial_x^2 u + \mu (\partial_x u)^2 \right]. \quad (1)$$

*Corresponding author

**Principal corresponding author

Email address: `matvbg@uni-miskolc.hu` (Gabriella Bognár)

¹This is the specimen author footnote.

²Another author footnote, but a little more longer.

³Yet another author footnote. Indeed, you can have any number of author footnotes.

The unknown function $u(x, t)$ designates the amplitude of the unstable branch, t is the time and x is the coordinate along the step. Coefficients ν, μ and κ ($\kappa = 1$) are positive physical parameters.

Equations of the type (1) have been employed in different physical contexts. In Ref. [15], the authors mentioned that equation (1) is a possible (natural) candidate for the time-evolution of the meandering amplitude, if desorption is negligible.

The CKS equation, after rescaling, can be interpreted as a particular case ($\epsilon = 0$) of the following modified CKS equation

$$\partial_t u = -\partial_x^2 \left[u - \epsilon \partial_x u + \partial_x^2 u + \frac{1}{2} (\partial_x u)^2 \right]. \quad (2)$$

The above equation is used to describe bunches created by an electromigration current [16]. It is worth noticing that the term $\partial_x^3 u$ can be removed from equation (2) via transformation $u \rightarrow u - \epsilon x$. Equation (2) is also proposed in [17] to describe sand ripples formation close to the instability threshold.

In 2009, Politi and ben-Avraham [18] showed that the CKS equation can be mapped into the motion of a system of particles with attractive interactions, decaying as the inverse of their distance.

The following continuum d -dimensional model ($d = 1, 2$)

$$\partial_t u = -\Delta [\nu u + \kappa \Delta u + \mu |\nabla u|^2] \quad (3)$$

with positive coefficients ν, κ and μ , has been introduced by Raible et al. [19] in the context of amorphous thin film growth. The above equation is a closely related to a more general equation

$$\partial_t u = -\Delta [\nu u + \kappa \Delta u + \mu |\nabla u|^2] + \Lambda |\nabla u|^2, \quad (4)$$

or to the following equation

$$\partial_t u = -\Delta [u + \Delta u + r |\nabla u|^2] + |\nabla u|^2. \quad (5)$$

Equation (5), which is deduced from (4) with $r = \nu\mu/\kappa\Lambda$, appears in the context of ion beam sputtering (IBS). This equation is obtained by Castro et al. [20] from a two-dimensional (reaction and transport mechanisms) system of the coupled thickness of the mobility surfaces adatoms layer and the height of the bombarded surface u (see also [21] for one-dimension case). Note that for $r = 0$ equation (5) reduces to the famous Kuramoto-Sivashinsky equation which is known to produce spatio-temporal chaos. For $r \rightarrow \infty$ ($\Lambda \rightarrow 0$), we obtain equation (3) from (4). Therefore, one finds that r is a very important parameter, which determines the character of the solutions to equation (5).

Note that if $\kappa = \mu = 0$, equation (4) reads

$$\partial_t u = -\nu \Delta u + \Lambda |\nabla u|^2, \quad (6)$$

and then the new function $v \equiv -\frac{\Lambda}{\nu} u(x, -t/\nu)$ satisfies the well-known Kardar-Parisi-Zhang (KPZ) equation [22]

$$\partial_t v = \Delta v + |\nabla v|^2, \quad (7)$$

which has explicit solution [23] given by

$$v(x, t) = \ln \left(\frac{1}{4\pi t} \exp \left(-\frac{x^2 + y^2}{4t} \right) \right). \quad (8)$$

If $\nu = \Lambda = 0$ in (4), we obtain, as above, the conserved Kardar-Parisi-Zhang (CKPZ) equation

$$\partial_t v = \Delta (\Delta v + |\nabla v|^2). \quad (9)$$

Results, for the coarsening process, have been presented for (3) and (5) (see below), but do not seem to describe completely the dynamics. The aim of this work is to revisit, from the theoretical point of view, equations (3) and (5). In particular, we shall present results showing that surfaces can be mathematically and physically classified into different categories. Attention will be focused on the effect of the CKPZ term $\Delta(|\nabla u|^2)$ for equation (3) and the interplay between the CKPZ and the KPZ, $|\nabla u|^2$, terms for equation (5).

2. Analytical results

In this section we analyze equation (3) and for sake of comparison we consider equation (5) without the KPZ term:

$$\partial_t u = -\Delta [u + \Delta u + r|\nabla u|^2]. \quad (10)$$

For reader convenience, we analyze, as in [19], one and two dimensional cases separately applying similarity method. Then, the effect of the KPZ term is investigated.

2.1. One-dimensional problem

Here, we investigate the solutions of the conserved Kuramoto-Sivashinsky (CKS) equation in one dimension.

$$u_t + \frac{\partial}{\partial x^2} [u + u_{xx} + r(u_x)^2] = 0. \quad (\text{CKS-1})$$

As mentioned before the above equation was considered in [14]. Numerical solutions reveal that the typical length scale grows as $\lambda(t) \sim t^\beta$, with the coarsening exponent $\beta = 1/2$ (see also [16]). It is shown that the general asymptotic solution can be thought of as a superposition of parabolas. Similarity solutions are also considered. Trying the solution ansatz

$$u(t, x) = t^\alpha f(\eta), \quad \eta = xt^{-\beta}, \quad (11)$$

one obtains $\alpha = 1$, $\beta = 1/2$ and we get

$$f - \frac{1}{2}\eta f' + f'' + t^{-1}f'''' + r(f'^2)'' = 0, \quad (12)$$

where $' = df/d\eta$.

Note that at $t = 0$ we cannot eliminate u_{xxxx} . In general, there is no similarity solution.

If $t \rightarrow \infty$ then we suppose that $t^{-1}f'''' \rightarrow 0$. Particularly, if $f^{(4)} \equiv 0$, then $f = a\eta^3 + b\eta^2 + c\eta + e$. From equation (12) the coefficients in f are $a = 0$, $c = 0$, $e = e(b)$, with some $b < 0$, $e < 0$

$$\begin{aligned} u(x, t) &= t \left(b \frac{x^2}{t} - e \right) = bx^2 - et \\ &= -e \left(t - \frac{b}{e} x^2 \right)_+ \end{aligned} \quad (13)$$

From (13) one immediately sees that $\lambda(t) = 2\sqrt{\frac{e}{b}t}$ and $A(t) = |e|t$, i.e., $\alpha = 1$ and $\beta = 1/2$. We note that in [14], the authors obtained an explicit solution having the form $u_{\text{ex}}(x, t) = -x^2/(r4)$, for $|x| < \text{const.}\sqrt{t}$, and zero elsewhere. Explicit solution (13) and u_{ex} indicate that for any initial conditions $A(0)$ and $\lambda(0)$, the surface will grow without limit (uninterrupted coarsening), which is physically not correct.

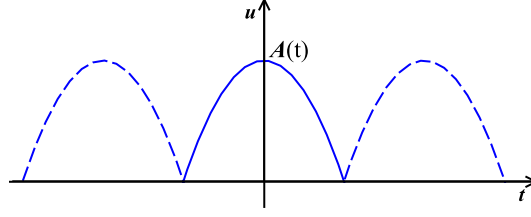


Figure 1: The height profile of $u(x, t)$

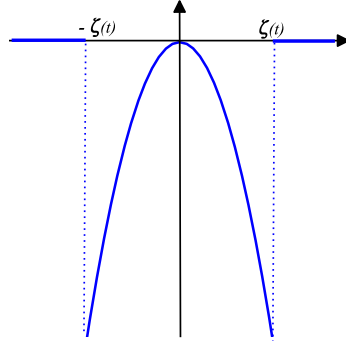


Figure 2: The height profile

Next, multiplying equation

$$u_t = -u_{xx} - u_{xxxx} - r \left((u_x)^2 \right)_{xx}$$

by u and integrating twice one gets

$$\frac{d}{dt} \frac{1}{2} \int_{\mathbf{R}} u^2 dx = \int_{\mathbf{R}} (u_x)^2 dx - \int_{\mathbf{R}} (u_{xx})^2 dx. \quad (14)$$

Shifting the maximum of the unsteady solution to $x = 0$ from equation (CKS-1) we get the form of u as

$$u(x, t) = \begin{cases} -\frac{1}{4r}x^2 & \text{if } |x| < \zeta(t), \\ 0 & \text{if } |x| \geq \zeta(t), \end{cases}$$

where $\zeta(t)$ is an unknown function (see Fig.2).

Substituting it into (14) we have

$$\frac{d}{dt} \int_0^{\zeta(t)} \frac{1}{8} x^4 dx = \int_0^{\zeta(t)} x^2 dx - \int_0^{\zeta(t)} dx$$

i.e., it is equivalent to

$$\frac{1}{8} \zeta^3(t) \zeta'(t) = \frac{1}{3} \zeta^2(t) - 1.$$

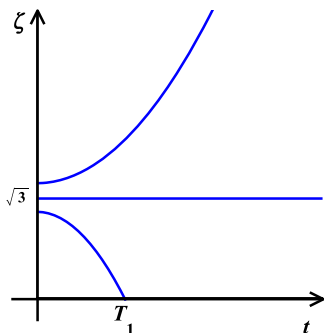


Figure 3: Solution $\zeta(t)$ for different values of $\zeta(0)$

The solution to this differential equation is given implicitly by

$$t = \frac{9}{16} \left[\frac{1}{3} \zeta^2(t) - \frac{1}{3} \zeta^2(0) + \ln \left| \frac{\frac{1}{3} \zeta^2(t) - 1}{\frac{1}{3} \zeta^2(0) - 1} \right| \right]$$

(see Fig.3) and $\zeta(t)$ vanishes at

$$T_1 = \frac{9}{16} \left[-\ln \left| \frac{1}{3} \zeta^2(0) - 1 \right| - \frac{1}{3} \zeta^2(0) \right]$$

if $\zeta(0) < \sqrt{3}$. Note, that $T_1 \rightarrow \infty$ as $\zeta(0) \rightarrow \sqrt{3}$.

If the initial wavelength $\lambda = 2\zeta(0)$ is larger than $2\sqrt{3}$, then the amplitude and the period growth without limit. In this case, the period behaves like \sqrt{t} (typical behavior) and the amplitude behave like t as t tends to ∞ .

The case $\lambda(0) = 2\sqrt{3}$ leads to a stationary periodic solution, i.e., $\lambda(t) = 2\sqrt{3}$, for all t .

It turns out that property (14), which played a crucial role in the time behavior of solutions, still valid even if the CKPZ term is not present. At first sight, we may deduce that the CKPZ term, which acts at small scales, has no effect on the time-behavior of the typical length.

2.2. Two-dimensional problem

Next, we investigate the nonlinear deterministic equation in two dimensions. Let us take the conserved Kuramoto-Sivashinsky equation as growth equation in the form

$$u_t + \Delta \left(u + \Delta u + r |\nabla u|^2 \right) = 0. \quad (\text{CKS-2})$$

We suppose that $\mathbf{x} \in \mathbf{R}^2$, and u is a C^2 smooth function. Multiplying (CKS-2) with u and integrating twice one gets

$$\begin{aligned} \frac{d}{dt} \frac{1}{2} \int_{\Omega} u^2 dx dy &= \int_{\Omega} |\nabla u|^2 dx dy \\ - \int_{\Omega} (\Delta u)^2 dx dy - r \int_{\Omega} |\nabla u|^2 \Delta u dx dy & \end{aligned} \quad (15)$$

for any rapidly decreasing solution u .

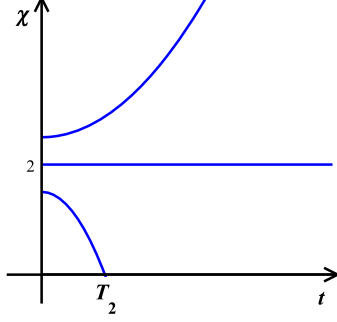


Figure 4: Function $\chi(t)$ for different initial values of $\chi(0)$

If u represents the mound like growth of the form of $u = C(x^2 + y^2)$ with some parameter $C < 0$, then one obtains from the partial differential equation (CKS-1) that

$$C = -\frac{1}{4r},$$

i.e.,

$$u = -\frac{1}{4r}(x^2 + y^2)$$

and

$$u(x, y, t) = \begin{cases} -\frac{1}{4r}(x^2 + y^2) & \text{if } x^2 + y^2 < \chi^2(t) \\ 0 & \text{if } x^2 + y^2 \geq \chi^2(t) \end{cases}$$

with some function χ . Then $\max |u| = \chi^2/4r$. Taking the integrals for $\Omega = B(0, \chi)$ in (15) we obtain the differential equation for χ

$$\frac{1}{8}\chi^3(t)\chi'(t) = \frac{1}{2}\chi^2(t) - 2. \quad (16)$$

By integration one gets the solution as

$$t = \frac{1}{2} \left[\frac{1}{4}\chi^2 - \frac{1}{4}\chi^2(0) + \ln \left| \frac{\frac{1}{4}\chi^2 - 1}{\frac{1}{4}\chi^2(0) - 1} \right| \right] \quad (17)$$

If $\chi(0) < 2$, then $\chi(t)$ collapses at finite T_2 , see Fig.4, where

$$T_2 = \frac{1}{2} \left[-\ln \left| \frac{\frac{1}{4}\chi^2(0) - 1}{-\frac{1}{4}\chi^2(0)} \right| - \frac{1}{4}\chi^2(0) \right]. \quad (18)$$

For $\chi(0) > 2$, the period and amplitude for large initial data behave like in the one-dimensional case, while if $\chi(0) = 2$ we obtain a stationary periodic solution.

2.3. The effect of the KPZ term

Next, we study analytically the effect of the nonlinear term in (CKS-2). As above we consider the two and one-dimensional cases separately; in two-dimension

$$u_t = -\Delta \left(|\nabla u|^2 \right) \quad (19)$$

and in one-dimension

$$u_t = -(u_x)_{xx}^2. \quad (20)$$

With substitution $v = u_x$ to equation (20) one gets

$$v_t = -(v^2)_{xxx}.$$

Self-similar solution for v can be searched in the form

$$v(x, t) = (T_3 - t)^\alpha g \left(x (T_3 - t)^{-\beta} \right),$$

for some T_3 . Then the differential equation (20) takes the form of

$$(g^2)''' - \alpha g + \beta \eta g' = 0$$

when

$$-\alpha + 3\beta = 1 \quad (21)$$

for $g = g(\eta)$ with $\eta = x (T_3 - t)^{-\beta}$. Physically, as we have conserved equation, we must have $\alpha + \beta = 0$, and therefore with (21) one gets $-\alpha = \beta = 1/4$. Then

$$\frac{1}{4}\eta g + (g^2)'' = K_1, \quad (22)$$

where K_1 is a constant.

(i.) If $K_1 = 0$ and $g(\eta) = C\eta^3$ then for (22) we get that $g = -\eta^3/120$ and

$$\begin{aligned} v &= -\frac{1}{120} (T_3 - t)^{-\frac{1}{4}} \left(x (T_3 - t)^{-\frac{1}{4}} \right)^3 \\ &= -\frac{1}{120} \frac{x^3}{T_3 - t}. \end{aligned}$$

Therefore solution u reads as

$$u = -\frac{1}{480} \frac{x^4}{T_3 - t} + K_2 \quad (23)$$

with some constant K_2 .

It is easy to see from (23) that the wavelength $\lambda = 2(480K_2(T_3 - t))^{1/4}$ collapses at finite time.

(ii.) The numerical solutions to equation (22) with initial conditions $f(0) = 1$, $f'(0) = 10$ can be obtained (see Fig.5).

(iii.) At $\eta = \eta_k$ the differential equation (22) behaves like

$$gg'' + g'^2 = 0. \quad (24)$$

For this equation the solution

$$g \sim \sqrt{\eta_k - \eta}$$

has vertical asymptote at η_k . Hence,

$$v \sim (T_3 - t)^{-\frac{1}{4}} \sqrt{\eta_k - x (T_3 - t)^{-\frac{1}{4}}} \quad (25)$$

and

$$u \sim \left[K_3 - \frac{2}{3} \left(\eta_k - x (T_3 - t)^{-\frac{1}{4}} \right)^{\frac{3}{2}} \right]_+ \quad (26)$$

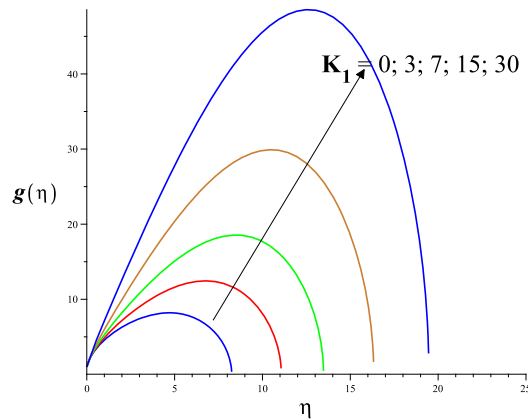


Figure 5: Solutions to (22) for different values of K_1

with a constant K_3 . Then, u collapses at finite time.

In case of two-dimensional problem (19), the solution u is searched in the form

$$u(x, y, t) = [a(T_4 - t) - b(x^2 + y^2)]_+ \quad (27)$$

for some constants a , b and T_4 . Substituting u into (19), we obtain $a = 16b^2$ and

$$u(x, y, t) = b(T_4 - t) \left[16b - \frac{x^2 + y^2}{T_4 - t} \right]_+, \quad (28)$$

this is precisely a similarity solution, which shows that both the amplitude $A = b(T_4 - t)$ and the wavelength $\lambda = 4\sqrt{b}\sqrt{T_4 - t}$ decrease with time and vanish at finite time T_4 . This may give some light to the qualitative effect of the CKPZ term on physical properties of the CKPZ equation. The aim of the next section is to investigate the effect of the KPZ term by using numerical solutions.

3. Numerical results

Both the one-dimensional and two-dimensional generalized Kuramoto-Sivashinsky equation are solved with periodic boundary conditions using Fourier spectral collocation in space and the fourth order Runge-Kutta exponential time differencing scheme for time discretization.

3.1. One-dimensional case

First, we investigate the one-dimensional generalized Kuramoto-Sivashinsky equation

$$u_t = -u_{xx} - u_{xxxx} + (u_x)^2 - r((u_x)^2)_{xx}, \quad (29)$$

$$x \in (x_1, x_2), \quad t > 0$$

with periodic boundary condition

$$u(x_1) = u(x_2) \quad (30)$$

for some points x_1 and x_2 and with initial condition

$$u(x, 0) = u_0(x). \quad (31)$$

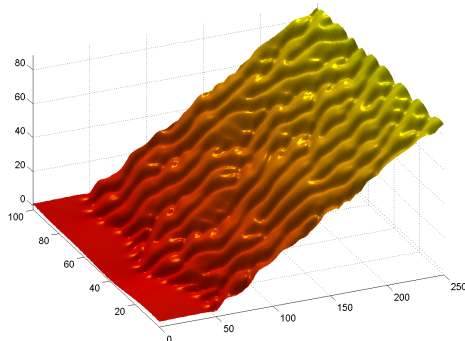


Figure 6: Solution to (29), (32) for $r = 0.01$ and $A(0) = 1$

Let us discretize function u of (29) in x for N equidistant points and then take its discrete Fourier transform. Taking the time derivative component-wise and using formula for the transform of the derivatives, we get from (29) a system of ordinary differential equations. Function $(u_x)^2$ is evaluated pseudospectrally in the Fourier space.

For temporal discretization of the system we apply the exponential time differencing method ETDRK4 scheme, a fourth order Runge-Kutta time stepping introduced by Cox and Matthews in [24]. The program for solving the IBVP (29)–(31) is created both in MATLAB (version R2011a) and in C++ using the ArrayFire library (version 3.0.1, build 17db1c9). In MATLAB, the default double precision type is used to be able to exploit the precision of the spectral method. In ArrayFire, the variables are declared as real and complex double precision types (`f64` and `c64` types, respectively).

In the one-dimensional case the initial condition used is of the form

$$u(x, 0) = A(0) \cos \frac{x}{16} \left(1 + \sin \frac{x}{16} \right), \quad (32)$$

where A is a positive constant. Figures 6-9 show the numerical solution for differently chosen r with parameters $N = 256$, $\Delta t = 1/100$ on $x \in [0, 32\pi]$, $t \in [0, 250]$. For contour integration with trapezoidal rule, $M = 32$ is applied.

The following consequences can be drawn from the figures. First, the increase of r causes the solution function u grow less, meaning that the accumulation of atoms on the surface is far less significant that for smaller r . Second, the chaotic nature of the solution emerges later in time when r is large. Third, the accumulation of the atoms to the surface starts later with smaller value of A (see Fig. 6 and 7). It is not seen in the figures, but the solution became bounded for a longer time interval when r was small. It can either be a numerical issue or the exact solution itself blows up at finite time; it needs further investigations.

Efficient MATLAB and ArrayFire codes were written to tackle the initial value problem numerically. The simulated results show physically meaningful characteristics and are similar to the results obtained with microscopic measurements.

3.2. Two-dimensional case

In case of the 2D problem, equation

$$u_t + \Delta (u + \Delta u + r|\nabla u|^2) = 0, \quad (x, y) \in (a, b)^2 \quad (33)$$

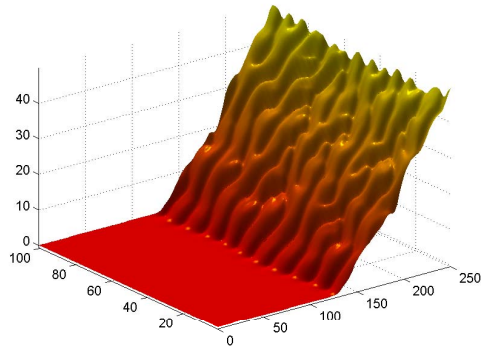


Figure 7: Solution to (29), (32) for $r = 0.01$ and $A(0) = 0.01$

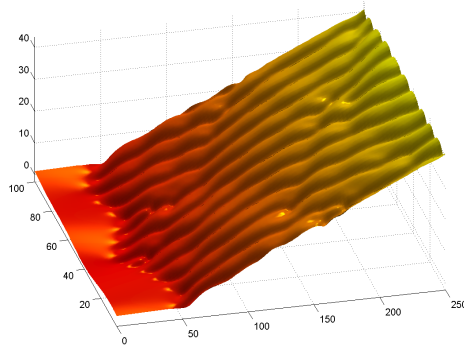


Figure 8: Solution to (29), (32) for $r = 0.5$ and $A(0) = 1$

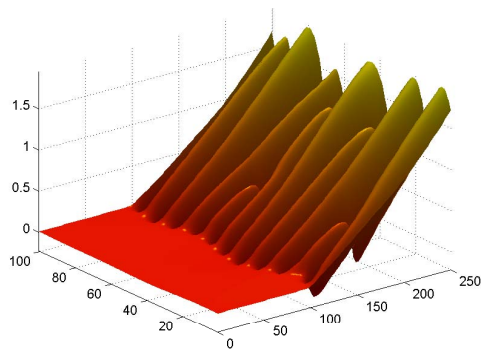


Figure 9: Solution to (29), (32) for $r = 10$ and $A(0) = 0.01$

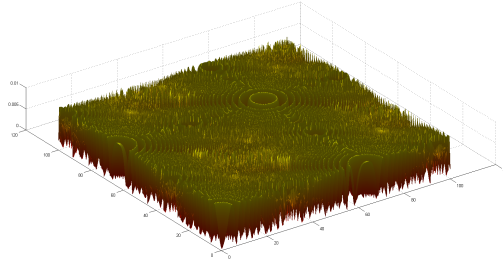


Figure 10: Solution to (33), (34) for $r = 10$ at $t = 0$

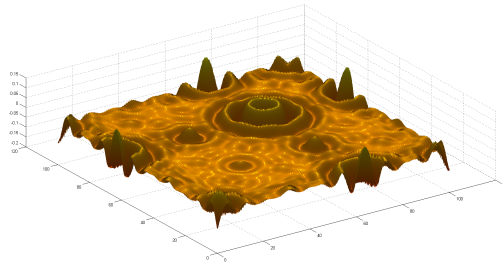


Figure 11: Solution to (33), (34) for $r = 10$ at $t = 20$

is solved with different initial conditions on $(x, y) \in [0, 32\pi]^2$ using parameters $r = 10$, $N = 256$, $\Delta t = 1/100$, $M = 32$. The following initial conditions are considered

$$u(x, y, 0) = 0.01 \left| \sin \frac{x^2 + y^2}{16} \right|, \quad (34)$$

$$u(x, y, 0) = 0.01 \left(\sin \frac{x^2 + y^2}{16} + \left| \sin \frac{x^2 + y^2}{16} \right| \right), \quad (35)$$

$$u(x, y, 0) = 0.1 \sin \frac{x^2}{16} \cos \frac{y^2}{16}. \quad (36)$$

The two-dimensional problem (33) is solved numerically with the initial condition

$$u(x, y, 0) = u_0(x, y). \quad (37)$$

The implementation of the two-dimensional case is similar to the one-dimensional one, because the two-dimensional discrete Fourier transform also results in decoupled ordinary differential equations. The only difference is that the unknowns now constitute a matrix instead of a vector as in the one-dimensional case. The temporal discretization schemes apply to scalar equations, therefore we can take the formulas component-wise as we did before.

Figures 10-12 depict the solution using the initial condition (34), Figs. 13-15 show it for (35) and Figs. 16-18 represent it with (36). The numerical solutions are exhibited at discrete time steps $t = 0$, $t = 20$ and $t = 30$.

Our first impression might be the jaggedness of the graph of the solution. It is so, because we did not use an aliasing method (like zero padding or phase shift). It is experienced from the

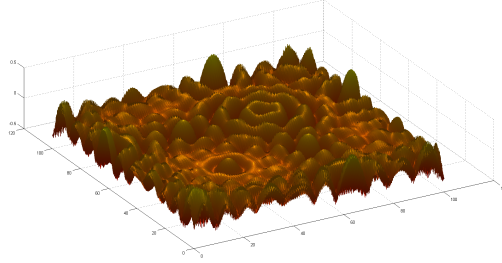


Figure 12: Solution to (33), (34) for $r = 10$ at $t = 30$

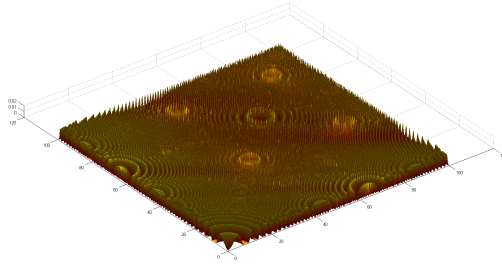


Figure 13: Solution to (33), (35) for $r = 10$ at $t = 0$

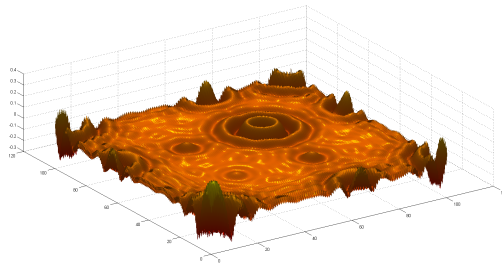


Figure 14: Solution to (33), (35) for $r = 10$ at $t = 20$

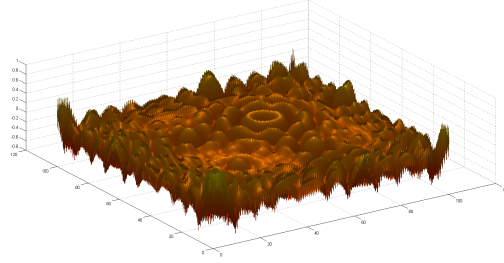


Figure 15: Solution to (33), (35) for $r = 10$ at $t = 30$

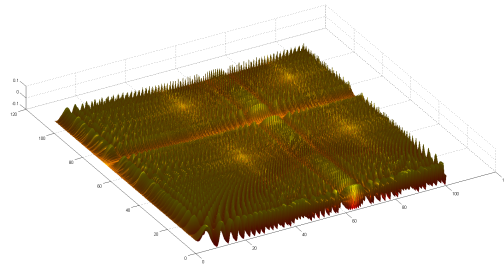


Figure 16: Solution to (33), (36) for $r = 10$ at $t = 0$

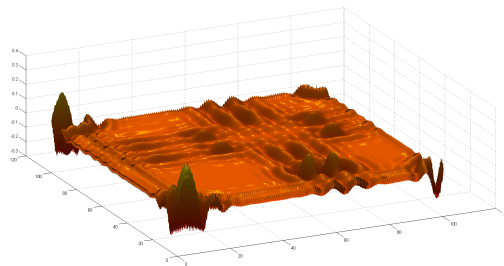


Figure 17: Solution to (33), (36) for $r = 10$ at $t = 20$

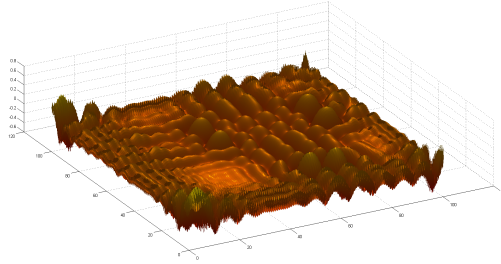


Figure 18: Solution to (33), (36) for $r = 10$ at $t = 30$

graphs that aliasing is much more prominent in case of the two-dimensional problem. With the decrease of parameter r in the nonlinear partial differential equation (33), the simulation became stable for longer time interval, similarly to the one-dimensional case.

4. Conclusion

We have analyzed one- and two-dimensional evolution equations in the context of amorphous thin film growth. It is found that the dynamics depends on the initial wavelength and amplitude. Three different behaviors are predicted. For large enough $\lambda(0)$ and $A(0)$, the surface growth without limit, and in this case $A(t)$ behaves like t and $\lambda(t)$ behaves like \sqrt{t} . If the initial wavelength $\lambda(0)$ is small enough, the surface collapses at finite time. This phenomena is a consequence of the presence of the nonlinear conserved KPZ term. At some critical value of λ , the surface structure does not change.

Some numerical solutions are presented for different value of parameters r and $A(0)$. For the same value of r , the surface with bigger $A(0)$ starts to grow earlier than the surface with smaller initial amplitude. For large r the surface exhibits the coarsening phenomena while for very small r the surface shows chaotic phenomena. Note, that if $r \rightarrow 0$ then equation (29) reduces to the Kuramoto-Sivashinsky equation, which exhibits spatiotemporal chaotic phenomena. The numerical simulations for two-dimension in case of $r = 10$ present the coarsening phenomena in agreement with the analytical result. Further analytical investigation will be done on the interplay between the conserved KPZ term and nonconserved KPZ term for general dimension D .

Acknowledgments

This research was supported by the European Union and the Hungarian State, co-financed by the European Regional Development Fund in the framework of the GINOP-2.3.4-15-2016-00004 project, aimed to promote the cooperation between the higher education and the industry. The authors acknowledge support by PHC-Balaton Number 34494UG, National Research, Development and Innovation Office within the TÉT_14_FR-1-2015-0004 project by 1.468 M Ft.

References

References

- [1] J. Villain, J. Phys. I France 1, 19 (1991).

- [2] G. Ehrlich, F. G. Hudda, *J. Chem. Phys.* 44, 1039 (1966).
- [3] R. L. Schwoebel, E. J. Shipsey, *J. Appl. Phys.* 37, 3682 (1966).
- [4] J. Krug, M. Plischke, M. Siegert, *Phys. Rev. Lett.* 70, 3271 (1993).
- [5] M. D. Johnson, C. Orme, A. W. Hunt, D. Graff, J. Sudijono, L. M. Sander, *Phys. Rev. Lett.* 72, 116 (1994).
- [6] O. Pierre-Louis, C. Misbah, Y. Saito, J. Krug, P. Politi, *Phys. Rev. Lett.* 80, 4221 (1998).
- [7] F. L. Forgerini, R. Marchiori, *Biomatter*, 4:e28871; PMID: 24751679 (2014)
- [8] J. Muñoz-García, L. Vázquez, M. Castro, R. Gago, A. Redondo-Cubero, A. Moreno-Barrado, R. Cuerno, *Mater. Sci. Eng. R Rep.* 86, 1 (2014)
- [9] J. W. Evans, P. A. Thiel, M. C. Bartelt, *Surface Science Reports* 61, 1 (2006).
- [10] I. Bena, C. Misbah, A. Valance, *Phys. Rev. B.* 47, 7408 (1993).
- [11] M. Uwaha, M. Sato, *Europhys. Lett.* 32, 639 (1995).
- [12] S. Paulin, F. Gillet, O. Pierre-Louis, C. Misbah, *Phys. Rev. Lett.* 86, 5538 (2001).
- [13] P. Politi, C. Misbah, *Phys. Rev. Lett.* 92, 090601 (2004).
- [14] T. Frisch, A. Verga, *Phys. Rev. Lett.* 96, 166104 (2006).
- [15] F. Gillet, O. Pierre-Louis, C. Misbah, *Europ. Phys. J. B.* 18, 519 (2000).
- [16] F. Gillet, Z. Csahok, C. Misbah, *Phys. Rev. B* 63, 241401 (2001).
- [17] Z. Csahok, C. Misbah, A. Valance, *Physica D* 128, 87 (1999).
- [18] P. Politi, D. ben-Avraham, *Physica D* 238, 156 (2009).
- [19] M. Raible, S. J. Linz, P. Hänggi, *Phys. Rev. E* 62, 1691 (2000).
- [20] M. Castro, R. Cuerno, L. Vázquez, R. Gago, *Phys. Rev. Lett.* 94, 016102 (2005).
- [21] J. Muñoz-García, R. Cuerno, M. Castro, *Phys. Rev. E* 74, 050103-1 (2006).
- [22] P. I. Tamborenea, Z.-W. Lai, S. Das Sarma, *Surface Science* 267, 1 (1994).
- [23] B. H. Gilding, M. Guedda, R. Kersner, *J. Math. Anal. Appl.* 284, 733 (2003).
- [24] S. M. Cox, P. C. Matthews. Exponential Time Differencing for Stiff Systems. *Journal of Computational Physics*, 176(2), 430 (2002).